# Magnetic vortices in a distributed Josephson junction with electrodes of finite thickness

G.L. Alfimov and A.F. Popkov
*F.V. Lukin's Research Institute of Physical Problems, Zelenograd, Moscow, 103460, Russia*
(Received 10 February 1995)

A distributed Josephson junction with electrodes of finite thickness is considered in the case of high critical current density when the Josephson penetration depth $\lambda_j$ is less than the London depth $\lambda_L$. A nonlinear nonlocal equation for steady-state distributions of phase difference $\varphi$ across the junction is derived. In the asymptotical case of thin electrodes an exact nonlinear solution for this equation which corresponds to an isolated at-rest Josephson vortex is found. A numerical investigation of the equation derived is carried out and some static and dynamic characteristics of vortices in such a Josephson junction are represented.

## I. INTRODUCTION

A distributed Josephson contact with a high density of critical current $j_s$ cannot be covered by the traditional sine-Gordon equation when a constant of magnetic field screening $\lambda_j$ in it is less than (or at least is comparable with) a London depth $\lambda_L$ of magnetic field penetration into the superconductor.[1–8] Magnetostatics and electrodynamics of the contact become nonlocal. Different reasons may cause this situation. First, the nonlocal model of the distributed Josephson junction can describe hidden defects in high-temperature oxide superconductors,[2] where the London screening depth is relatively large ($\lambda_L \sim 0.2$ $\mu$m) and the coherence length is very small ($\xi \sim 0.4$–$2.0$ nm). In this situation the critical current $j_s$ through weak links bounded by depairing currents in the superconductors ($j_s < j_d \sim 10^7$–$10^8$A/cm$^2$) can vary over a wide range and the condition

$$\xi \ll \lambda_j = \sqrt{\frac{c\Phi_0}{16\pi^2\lambda_L j_s}} \ll \lambda_L$$

can take place. Here $c$ is the speed of light and $\Phi_0$ is a magnetic flux quantum. Second, a violation of local electrodynamics in the distributed Josephson contact may occur under strong magnetic fields, approaching a lower critical field $H_{c1}$ of a bulk superconductor. In this case a longitudinal modulation of the phase difference at the junction caused by screening currents may have a period comparable with the London depth $\lambda_L$ and this may lead to the occurrence of nonlocal electrodynamics. The mechanisms mentioned for the occurrence of nonlocal Josephson electrodynamics were discussed in Refs. 1, 2, 4, and 6 in the ideal case of a junction with infinitely thick superconductive electrodes. At the same time, following Ref. 6 one would expect that the electrodynamics of the Josephson junction formed by thin ("transparent") electrodes may become nonlocal quite naturally. This is caused by the fact that when the thickness $d$ decreases the effective screening depth in thin films increases according to the formula $\lambda_{\text{eff}}^{(L)} = \lambda_L^2/d$.[9] At the same time the Josephson screening depth diminishes according to the relation $\lambda_{\text{eff}}^{(j)} \sim \sqrt{d}$. (see Ref. 10) The discussion of this situation for a single-layer thin superconductive film separated by a weak link is contained in Ref. 7 (a similar problem was considered recently in Ref. 8). However, no such consideration has been given in the literature for a non-one-layered structure of a distributed Josephson junction with thin electrodes.

The transition to a nonlocal model leads to various unusual consequences. For example a modification of the asymptotics of the dispersion relation in the short-wavelength range occurs; this implies a modification of the spectral characteristics of the junction radiation.[3,5,11] Another consequence of the transition to nonlocal model discussed in Ref. 2 is the modification of the structure of the magnetic vortex, which approaches the structure of an Abrikosov vortex as the Josephson screening depth $\lambda_j$ decreases. In the intermediate region $\lambda_L > \lambda_j \gg \sqrt{\lambda_L\xi}$ the magnetic vortex has no normal core yet and it turns out to be possible to modify the equation for the phase difference $\varphi(y)$ for its description. An explicit solution of this modified equation[2] shows that the characteristic size of the vortex core becomes equal to $l = \lambda_j^2/\lambda_L$. The modification of vortex characteristics may change the temperature dependence of the critical current, which is determined by a pinning of magnetic vortices, noise characteristics of weak links, etc.

In this paper the effect of finite thickness of the superconductive electrodes of the distributed Josephson junction on its magnetostatic and the structure features of a magnetic vortex is considered. The paper is organized as follows. In Sec. II a nonlocal equation is derived, which describes the distribution of the phase difference within the Josephson junction with superconductive electrodes of finite thickness (see Fig. 1). Supposing that the electrodes are sufficiently thin, an exact solution of this equation is obtained. Results of a numerical investigation for this equation are presented in Sec. III.

 

## II. BASIC EQUATIONS

Let us consider a thin Josephson contact of infinite length being formed by two identical electrodes of thickness $d$, which are situated on each side of the plane $x = 0$ (Fig. 1). Let us suppose that the contact is in static equilibrium. We assume that magnetic field $\vec{H}$ is parallel to the $z$ axis; in this case the components of the field and the screening current $\vec{J}$ are independent of the coordinate $z$:

$$\vec{H} \equiv \vec{H}(y,x) = (0,0,H_z), \qquad \vec{J} \equiv \vec{J}(y,x) = (J_x, J_y, 0).$$

Let us suppose that the magnetic field is homogeneous at an infinite distance from the contact plane,

$$H_z(y,x) \overset{x\to\infty}{\longrightarrow} H_\infty. \tag{1}$$

Furthermore, at the external boundaries of the superconductor the field continuity conditions hold:

$$H_z\big|_{x=\pm d+0} = H_z\big|_{x=\pm d-0}. \tag{2}$$

Let us assume that the distribution of the screening current $J_y(y,x)$ is antisymmetric with respect to $x$ and the thickness of the oxide layer $t$ is very small, $t \ll \lambda_L$. Moreover, we shall assume below that $t \to 0$. Integrating the expression for the superconductive current ($\vec{A}$ is vector of magnetic potential),

$$\vec{J} = \frac{c\Phi_0}{8\pi^2\lambda_L^2}\vec{\nabla}\varphi - \frac{c}{4\pi\lambda_L^2}\vec{A},$$

over the contour $\Gamma$ shown in Fig. 1, passing to the limit $\Delta y \to 0$, and putting $t = 0$ we obtain the boundary condition

$$J_y\big|_{x=+0} = \frac{c\Phi_0}{16\pi^2\lambda_L^2}\frac{\partial\varphi}{\partial y} = -J_y\big|_{x=-0}. \tag{3}$$

The component $J_x$ is related to $\varphi$ by means of the Josephson formula

$$J_x\big|_{x=0} = J_s \sin\varphi. \tag{4}$$

Furthermore, this component of the current vanishes at the external boundaries of the superconductors:

$$J_x\big|_{x=\pm d} = 0. \tag{5}$$

The magnetic field and the currents inside the superconductors are connected by means of London's equation and the equations of magnetostatics:

$$\mathrm{rot}\vec{H} = \frac{4\pi}{c}\vec{J}, \tag{6}$$

$$\mathrm{div}\vec{H} = 0, \tag{7}$$

$$\vec{H} = -\frac{4\pi\lambda_L^2}{c}\mathrm{rot}\vec{J}. \tag{8}$$

It follows that the superconductive current satisfies the equation

$$(\partial_x^2 + \partial_y^2 - 1/\lambda_L^2)\vec{J} = 0. \tag{9}$$

We will search the solutions of Eqs. (6)–(9) with the boundary conditions (1)–(5) in the form

$$\vec{J} = \vec{j}(y,x) + \vec{j}_\infty(x),$$

$$\vec{H} = \vec{h}(y,x) + \vec{h}_\infty(x), \tag{10}$$

where $\vec{j}_\infty$ and $\vec{h}_\infty$ are homogeneous along the junction and are represented by the expressions

$$\vec{h}_\infty(x) = (0,0,h_\infty(x)), \tag{11}$$

$$h_\infty(x) = \begin{cases} H_\infty \dfrac{\cosh(x/\lambda_L)}{\cosh(d/\lambda_L)}, & |x| < d, \\ H_\infty, & |x| > d, \end{cases}$$

$$\vec{j}_\infty(x) = (0, j_\infty(x), 0),$$

$$j_\infty(x) = \frac{cH_\infty}{4\pi\lambda_L}\frac{\sinh(x/\lambda_L)}{\cosh(d/\lambda_L)}, \qquad |x| < d. \tag{12}$$

At the same time the solutions $\vec{j}(y,x)$ and $\vec{h}(y,x)$ have to satisfy Eqs. (6)–(9), the boundary conditions (3) and (4) on the plane $x = 0$, and the zero boundary conditions at $x = \pm d$ for the current (5) and for the field:

$$h\big|_{|x|=d} = 0. \tag{13}$$

To find $\vec{j}(y,x)$ and $\vec{h}(y,x)$ we will use the Fourier transformation with respect to $y$:

$$\vec{j}(y,x) = \int_{-\infty}^{+\infty} \vec{j}^{\,k}(x) e^{iky} dk.$$

The solution required has the form

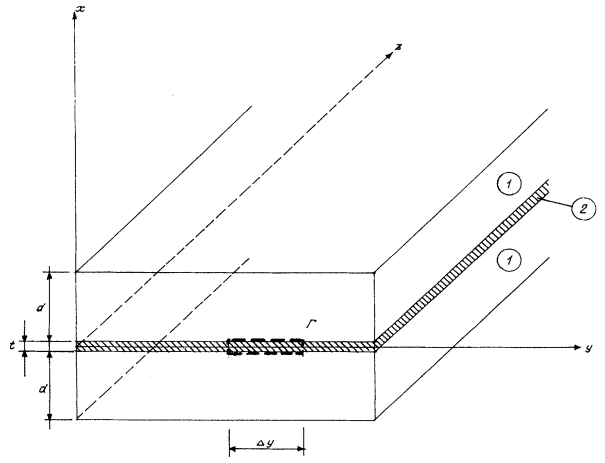


FIG. 1. Scheme of a Josephson junction: 1, superconductor; 2, tunnel layer.

$$j_x^k(x) = -j_y^k(0)\frac{ik\lambda_L}{\sqrt{1+k^2\lambda_L^2}}\,\frac{\sinh\{(d-|x|)\sqrt{1+\lambda_L^2k^2}/\lambda_L\}}{\cosh\{d\sqrt{1+\lambda_L^2k^2}/\lambda_L\}}, \tag{14}$$

$$j_y^k(x) = j_y^k(0)\frac{\cosh\{(d-|x|)\sqrt{1+\lambda_L^2k^2}/\lambda_L\}}{\cosh\{d\sqrt{1+\lambda_L^2k^2}/\lambda_L\}}\mathrm{sgn}x, \tag{15}$$

$$h_z^k(x) = j_y^k(0)\frac{4\pi\lambda_L}{c\sqrt{1+k^2\lambda_L^2}}\,\frac{\sinh\{(d-|x|)\sqrt{1+\lambda_L^2k^2}/\lambda_L\}}{\cosh\{d\sqrt{1+\lambda_L^2k^2}/\lambda_L\}}. \tag{16}$$

It is evident from the solution obtained that at the boundaries of the superconductive electrodes ($|x| = d$) $h_z^k(x)$ vanishes. Thus, it follows from the Maxwell equations with the boundary conditions (13) that outside the electrodes ($|x| > d$) the magnetic field $h(x,y) \equiv 0$. It is easy to conclude from (14) and (15) that the following relation between the normal and tangential components of the current is true:

$$j_x^k(x) = -j_y^k(x)\frac{ik\lambda_L}{\sqrt{1+k^2\lambda_L^2}}\,\tanh\left\{\frac{(d-|x|)}{\lambda_L}\sqrt{1+\lambda_L^2k^2}\right\}\mathrm{sgn}(x). \tag{17}$$

After the inverse Fourier transformation and taking into account the boundary conditions (3) and (4) we obtain the equation required for the phase difference across the junction:

$$\sin\varphi = \frac{\lambda_j^2}{\lambda_L}\int_{-\infty}^{\infty} G_\beta\left(\frac{|y-u|}{\lambda_L}\right)\frac{d^2\varphi}{du^2}du. \tag{18}$$

The kernel of the integral operator is determined by the Fourier integral

$$G_\beta(v) = \frac{1}{2\pi}\int_{-\infty}^{\infty}\frac{\tanh(\beta\sqrt{1+k^2})}{\sqrt{1+k^2}}\exp(ikv)dk, \tag{19}$$

where $\beta = d/\lambda_L$. One can show that the kernel (19) can be represented by means of the residues theory as the series

$$G_\beta(v) = \frac{1}{\beta}\sum_{n=0}^{\infty}\frac{\exp\{-\sqrt{1+(\frac{\pi}{2\beta})^2(1+2n)^2}|v|\}}{\sqrt{1+(\frac{\pi}{2\beta})^2(1+2n)^2}}. \tag{20}$$

Introducing the variable $w = y/\lambda_j$ it is possible to rewrite the equation (18) in the dimensionless form

$$\sin\varphi = \frac{1}{\mu}\int_{-\infty}^{\infty} G_\beta\left(\frac{|w-u|}{\mu}\right)\frac{d^2\varphi}{du^2}du, \tag{21}$$

where $\mu = \lambda_L/\lambda_j$. Being written in this form the equation involves two external parameters $\mu$ and $\beta$ only.

Let us consider some asymptotic cases of Eq. (18).

(a) In the asymptotic case of a large Josephson length $\lambda_j$ ($\mu = \lambda_L/\lambda_j \ll 1$), Eq. (18) turns into the classic sine-Gordon equation with a renormalized depth of the magnetic field screening. Using the properties of the Fourier transformation it is easy to check that when $\mu \to 0$, $\mu^{-1}G_\beta(|w-u|/\mu) \to (\tanh\beta)\delta(w-u)$ where $\delta$ is the Dirac function. So we can conclude that in the local limit $\mu \to 0$ the initial equation (18) takes the form

$$\sin\varphi = (\lambda_{\mathrm{eff}}^{(j)})^2\frac{d^2\varphi}{dy^2}; \qquad \lambda_{\mathrm{eff}}^{(j)} = \lambda_j\sqrt{\tanh(d/\lambda_L)}. \tag{22}$$

This asymptotics for the Josephson screening depth is in agreement with results of Refs. 10 and 12. A well-known solution of this equation is

$$\varphi(y) = 4\arctan(\exp\{\pm y/\lambda_{\mathrm{eff}}^{(j)}\}). \tag{23}$$

This solution describes the distribution of the phase difference within an isolated Josephson magnetic vortex.

(b) In the case of a large thickness of electrodes (when $\beta = d/\lambda_L \gg 1$) the following relation holds:

$$G_\beta(v) \simeq \frac{1}{2\pi}\int_{-\infty}^{\infty}\frac{\exp(ikv)}{\sqrt{1+k^2}}dk = K_0(v). \tag{24}$$

Here $K_0(v)$ is the McDonald function. In this limit the equation obtained coincides with the nonlocal magnetostatic equation for a distributed Josephson junction being derived in Refs. 1 and 2. In the case of strong nonlocality ($\lambda_j/\lambda_L \ll 1$) this equation has an approximate solution[2] describing an isolated magnetic vortex:

$$\varphi(y) \simeq \pi \pm 2\arctan(\lambda_L y/\lambda_j^2). \tag{25}$$

(c) Let us consider the case of the thin electrode limit $d \ll \lambda_L$ ($\beta \ll 1$). As this takes place the series (20) can be summed up and the kernel (19) takes the form

$$G_\beta(v) \simeq \frac{1}{\pi}\ln\coth\left(\frac{\pi}{4\beta}|v|\right). \tag{26}$$

Integrating by parts the right side of Eq. (18) we obtain

$$\sin\varphi = \frac{\lambda_j^2}{2\lambda_L d}\int_{-\infty}^{\infty}\frac{1}{\sinh\left(\frac{\pi(u-y)}{2d}\right)}\frac{d\varphi}{du}du, \tag{27}$$

where the integral means the principal value of the Cauchy integral. An equation similar to (27) arises in the dislocation theory for the description of elastic deformations induced by the Peierls dislocation in a plate of finite thickness.[13] Equation (27) admits an exact solution which corresponds to a solitary at-rest magnetic vortex. It has the form

$$\varphi(y) = \pi \pm 2\arctan\left[\frac{\sinh\frac{\pi y}{2D}}{\cos\frac{\pi d}{2D}}\right], \tag{28}$$

where the parameter $D$ is the greatest positive root of the transcendent equation

$$\cot\frac{\pi d}{2D} = \frac{\lambda_j^2\pi}{2D\lambda_L}. \tag{29}$$

The parameter $D$ determines the characteristic size of the vortex along the junction. It is possible to check that (28) is a solution of (27) by means of its direct substitution into the equation. In doing so the calculations become simpler if one operates with the Fourier transforms of the relations (27) and (28).

The phase distribution (28) allows us to find the distribution of currents and magnetic fields within the vortex. Using the Fourier transforms (14)–(16) and taking into account the formula

$$j_y^k(0) = -\frac{ik\lambda_j^2 j_s}{\lambda_L}\varphi^k,$$

where $\varphi^k$ is the Fourier transform of (28) we obtain after the integration

$$\frac{j_x}{j_s} \simeq \frac{2\pi\lambda_j^2}{\lambda_L D}\,\frac{\sin\frac{\pi(d-|x|)}{2D}\sinh\frac{\pi y}{2D}}{\cosh\frac{\pi y}{D} - \sin\frac{\pi(d-|x|)}{D}},$$

$$\frac{j_y}{j_s} \simeq \frac{2\pi\lambda_j^2}{\lambda_L D}\,\frac{\cos\frac{\pi(d-|x|)}{2D}\cosh\frac{\pi y}{2D}}{\cosh\frac{\pi y}{D} - \sin\frac{\pi(d-|x|)}{D}}\,\mathrm{sgn}x, \tag{30}$$

$$\frac{h_z c}{4\pi j_s\lambda_L} \simeq \frac{\lambda_j^2}{\lambda_L^2}\,\ln\frac{\cosh\frac{\pi y}{2D} + \sin\frac{\pi(d-|x|)}{2D}}{\cosh\frac{\pi y}{2D} - \sin\frac{\pi(d-|x|)}{2D}}.$$

The solutions represented above obey the Maxwell equations (6) and (7) but they do not satisfy the London equation (8) rigorously because they are asymptotic ones in the limit $d/\lambda_L \ll 1$. The structure of the magnetic vortex under different values of the external magnetic field is shown in Fig. 2. This figure shows how the external magnetic field penetrates into the thin electrodes of the Josephson junction which contains the magnetic vortex. There exists the value of the field, namely,

$$H_\infty = \frac{8\pi^2\lambda_j^2 j_s}{Dc}\,\frac{\cosh\frac{\pi d}{2D}}{\cosh\frac{\pi d}{D}}\,\coth\frac{d}{\lambda_L},$$

when the screening Meissner currents $j_\infty(x = d)$ at the external surface of the electrode compensate the vortex current $j_y(x = d, y = 0)$. Another critical value of the field is

$$H_\infty^0 = \frac{4\pi j_s\lambda_j^2}{\lambda_L c}\,\frac{\cosh(d/\lambda_L)}{2\sinh^2(d/2\lambda_L)}\,\ln\left[\frac{1+\sin(\pi d/2D)}{1-\sin(\pi d/2D)}\right], \tag{31}$$

when the value of the magnetic field in the vortex center is equal to the external field $H_\infty$. The value $H_\infty^0$ plays the role of the first critical field of the vortex penetration into the junction through its edge. The stability of the structures represented in Fig. 2 needs to be investigated.

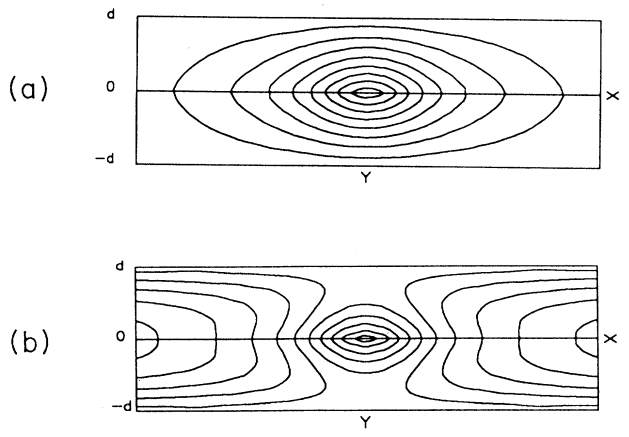


FIG. 2. A distribution of magnetic field within the junction. (a) $H_\infty = 0$, (b)$H_\infty > 0$.

## III. NUMERICAL INVESTIGATIONS: STATIC AND DYNAMIC PARAMETERS OF THE JOSEPHSON VORTEX

When the asymptotic approximations (a), (b), and (c), above, are inapplicable it seems reasonable to use numerical methods for the investigation of Eq. (18). Being written in the dimensionless form (21) the basic equation depends on the two parameters $\mu = \lambda_L/\lambda_j$ and $\beta = d/\lambda_L$ only. In this section we describe a modification of the form and characteristics of the single fluxon under a variation of these parameters and clarify the range where the asymptotic formulas (23),(25),(28) are applicable for its description.

To control the accuracy of the numerical calculations we used the fact that Eq. (21) possesses the first integral

$$I = (1-\cos\varphi) - \frac{1}{\mu^2}\int\int_{\substack{w'>w\\ w''<w}} G_\beta{}'\left(\frac{w'-w''}{\mu}\right) \times\frac{d\varphi}{dw'}\frac{d\varphi}{dw''}dw'dw''. \tag{32}$$

To verify the existence of this integral it is sufficient to differentiate the formula (32) and to use the fact that $\varphi$ is a solution of (21). It is necessary to point out that the existence of such an integral follows immediately from the results of Ref. 14 where a dynamical interpretation for nonlocal equations of this kind was suggested (see the Appendix). Let us note that the solitary fluxon solution corresponds to the zero level of the integral, $I = 0$. A deviation of $I$ from zero being calculated for the fluxon solution obtained numerically reveals a magnitude of the calculation error.

Figures 3 and 4 demonstrate the profiles of the phase difference distribution $\varphi(w) \equiv \varphi(y/\lambda_j)$ for the Josephson

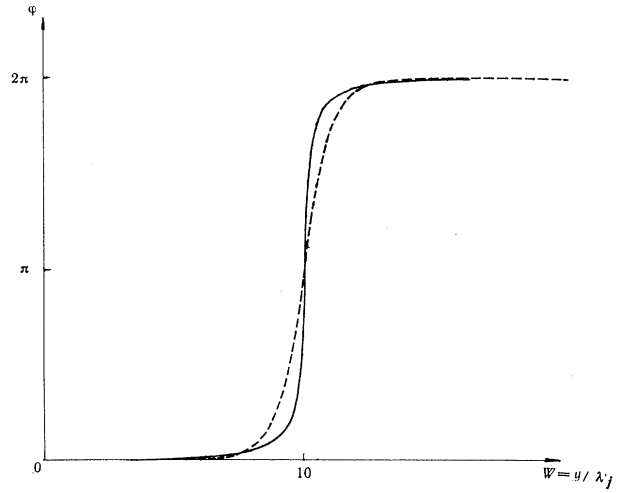


FIG. 3. The phase difference distributions $\varphi(w) = \varphi(y/\lambda_j)$ within the fluxon, $\beta = 0.5$; dashed line, $\mu = 0.1$; solid line, $\mu = 5$.

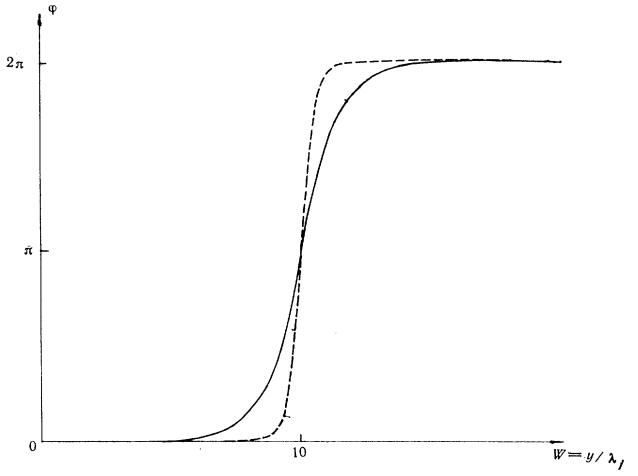


FIG. 4. The phase difference distributions $\varphi(w) = \varphi(y/\lambda_j)$ within the fluxon, $\mu = 0.5$; dashed line, $\beta = 0.1$; solid line, $\beta = 3$.

vortex obtained numerically under different values of $\beta$ and $\mu$. It can be seen from Fig. 3 that a decrease in the Josephson depth $\lambda_j$ under fixed values of $\lambda_L$ and $d$ leads to a shrinking of the vortex core and simultaneously to a dilatation of its periphery. On the other hand, Fig. 4 exhibits that a decreasing of electrode thickness $d$ leads to a shrinking of the vortex as a whole.

Let us discuss now some characteristics of the magnetic vortex related to its structure. Namely, let us calculate the energy of the magnetic vortex at zero external magnetic field and its mass and mobility in an adiabatic approximation. In the absence of an external magnetic field, $H_\infty = 0$, the free energy functional for the distributed junction can be represented as[4]

$$F = \frac{\Phi_0^2}{32\pi^3\lambda_j^2\lambda_L}\left\{\int_{-\infty}^{\infty}(1-\cos\varphi)dy + \frac{\lambda_j^2}{2\lambda_L}\int_{-\infty}^{\infty}\int_{-\infty}^{\infty}G_\beta\left(\frac{|y-u|}{\lambda_L}\right)\frac{d\varphi}{dy}\frac{d\varphi}{du}dydu\right\} \equiv F_0 J_1(\beta,\mu), \tag{33}$$

where $F_0 = \Phi_0^2/32\pi^3\lambda_L^2$ and the functional $J_1(\beta,\mu)$ is determined by the formula

$$J_1(\beta,\mu) = \frac{1}{2\pi}\left\{\mu\int_{-\infty}^{\infty}(1-\cos\varphi)dw + \frac{1}{2}\int_{-\infty}^{\infty}\int_{-\infty}^{\infty}G_\beta\left(\frac{|w-u|}{\mu}\right)\frac{d\varphi}{du}\frac{d\varphi}{dw}dudw\right\}. \tag{34}$$

Here $\varphi(w) \equiv \varphi(y/\lambda_j)$ is the distribution of the phase difference within the Josephson vortex. Figure 5 represents the curves for the dependence of the vortex energy $J_1(\beta,\mu) = F/F_0$ on the nonlocality parameter $\mu$ under different values of the parameter $\beta$ corresponding to the electrode thickness. Let us note that in the local limit $\mu \to 0$ $J_1(\beta,\mu) \approx 4\mu\sqrt{\tanh\beta}/\pi$. It is evident from Fig. 5 that the vortex energy grows when either the parameter $\mu$ or $\beta$ increases. The corresponding curves obtained for small $\beta$ by means of the formula (28) are depicted in the same figure for comparison. In this case the dependence $J_1(\beta,\mu)$ has the form

$$J_1(\beta,\mu) \approx \frac{1}{\pi}\Phi\left(\frac{\pi\beta\mu}{K}\right) + \frac{\beta\mu}{K}, \tag{35}$$

where $K$ is the greatest positive root of the transcendent equation

$$\cot\frac{\pi\beta\mu}{2K} = \frac{\pi}{2K\mu} \tag{36}$$

and $\Phi(\Delta) = \int_0^\Delta \frac{\theta}{\sin\theta}d\theta$ is the function which can be easily tabulated (see Table I). A comparison shows that a good agreement between numerical and asymptotical results

TABLE I. Values of the function $\Phi(\Delta) = \int_0^\Delta \frac{\theta}{\sin\theta}d\theta$.

| $\Delta$ | 0 | $\pi/20$ | $2\pi/20$ | $3\pi/20$ | $4\pi/20$ | $5\pi/20$ | $6\pi/20$ |
|---|---|---|---|---|---|---|---|
| $\Phi$ | 0 | 0.157 | 0.316 | 0.477 | 0.643 | 0.814 | 0.992 |
| $\Delta$ | $7\pi/20$ | $8\pi/20$ | $9\pi/20$ | $10\pi/20$ | $11\pi/20$ | $12\pi/20$ | $13\pi/20$ |
| $\Phi$ | 1.180 | 1.381 | 1.597 | 1.832 | 2.092 | 2.384 | 2.719 |
| $\Delta$ | $14\pi/20$ | $15\pi/20$ | $16\pi/20$ | $17\pi/20$ | $18\pi/20$ | $19\pi/20$ | $\pi$ |
| $\Phi$ | 3.110 | 3.582 | 4.174 | 4.960 | 6.105 | 8.144 | $\infty$ |

for $J_1(\beta,\mu)$ (up to 2%) takes place when $\beta \leq 0.3$ (at $\beta = 0.1$ the corresponding curves are indistinguishable).

It follows from Fig. 5 that under $\beta \geq 2$ and arbitrary values of $\mu$ an approximation of "infinitely thick" electrodes[1,2] can be applied successfully. Curve 4 represents the dependence $J_1$ on $\mu$ in this case. When $\beta \geq 2$ the values $J_1(\beta,\mu)$ coincide with this asymptotics with high accuracy; the corresponding curves in Fig. 5 are indistinguishable. At large values of $\mu$ and $\beta \geq 2$, the following formula corresponding to the nonlocal fluxon (25) can serve as a good approximation (see Ref. 6):

$$J_1 \simeq \gamma + 2\ln\mu, \qquad \gamma \approx 0.4228. \tag{37}$$

Let us turn to the discussion of some dynamical parameters of the vortex which can be obtained in an adiabatic approximation. We suppose that the fluxon velocity is small with respect to the velocity of light in the junction and the form of the fluxon suffers a weak distortion. Under these conditions it is possible to calculate the viscosity $\eta$ and mass $m$ of the fluxon which characterize the mobility and inertia of the vortex, respectively. In a zeroth approximation with respect to velocity these parameters are determined by the expressions (see, for example, Ref. 2)

$$\eta = \frac{\hbar^2\mu}{4e^2R\lambda_L}J_2(\beta,\mu), \tag{38}$$

$$m = \frac{\hbar^2 C\mu}{4e^2\lambda_L}J_2(\beta,\mu), \tag{39}$$

where $J_2(\beta,\mu) = \int_{-\infty}^{\infty}\left(\frac{d\varphi}{dw}\right)^2 dw$ and $C$ and $R$ are the linear capacity and resistance of the junction, respectively. Figure 6 exhibits the dependence of the functional $J_2(\beta,\mu)$ on the nonlocality parameter $\mu$ under different values of the normalized thickness of electrodes $\beta$. It can be concluded from Fig. 6 that when $\beta$ grows the vis-

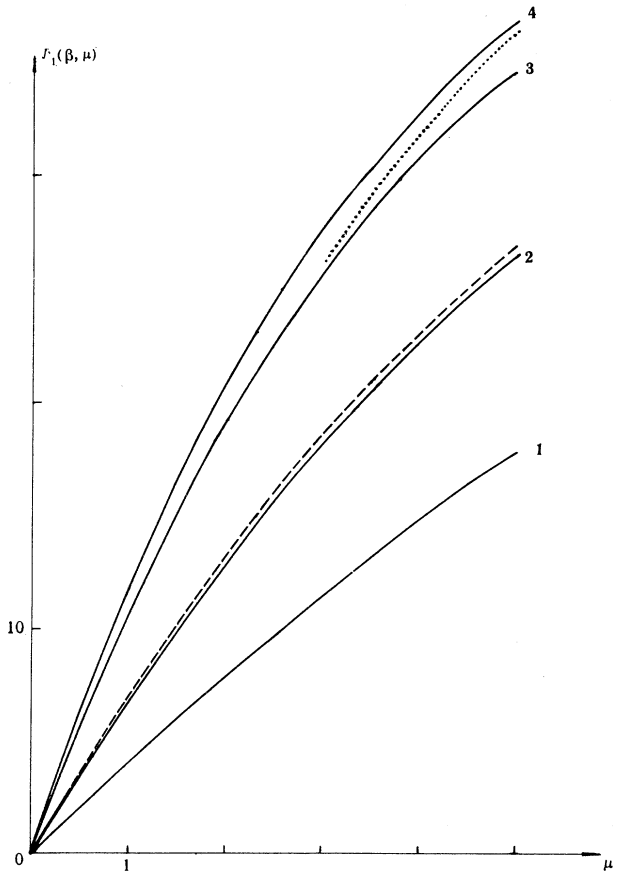


FIG. 5. The dependence of the functional $J_1(\beta,\mu)$ on the nonlocality parameter $\mu$ under different values of $\beta$. (1) $\beta = 0.1$, (2) $\beta = 0.3$, (3) $\beta = 1$, (4) $\beta = \infty$. Dashed line, the asymptotical dependence (35) for $\beta = 0.3$. Dotted line, the asymptotical dependence (37) corresponding to (25).

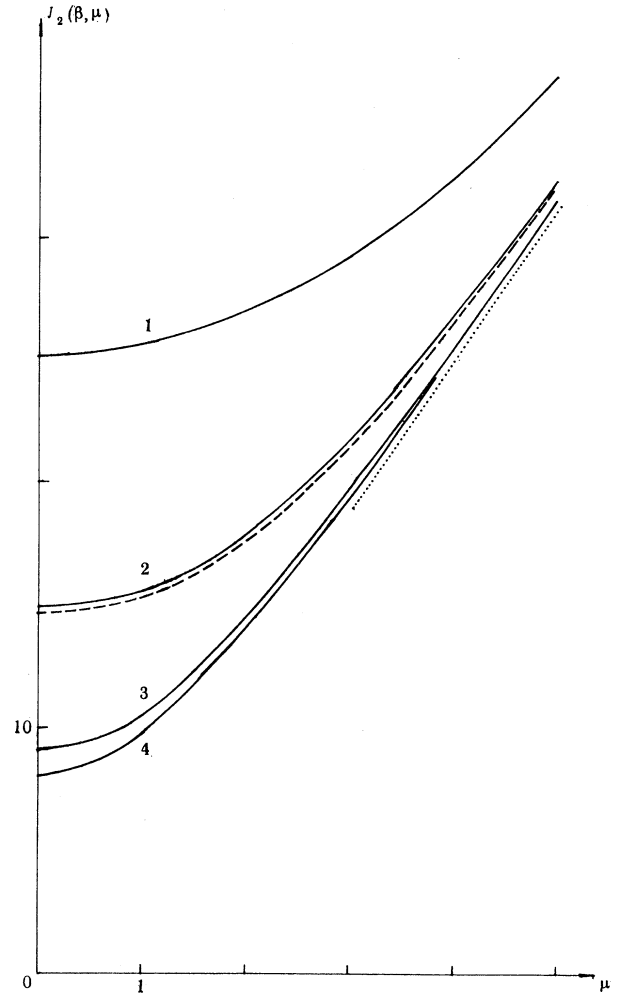


FIG. 6. The dependence of the functional $J_2(\beta,\mu)$ on the nonlocality parameter $\mu$ under different values of $\beta$. (1) $\beta = 0.1$, (2) $\beta = 0.3$, (3) $\beta = 1$, (4) $\beta = \infty$. Dashed line, the asymptotical dependence (40) for $\beta = 0.3$. Dotted line, the asymptotical dependence $J_2 \simeq 2\pi\mu$, $\mu \gg 1$ corresponding to (25).

cosity and the mass of the vortex decrease and, on the contrary, when $\mu$ grows they increase. When $\mu$ is small, $\mu \leq 0.5$, the local model (22) gives a good approximation for $J_2(\beta,\mu)$. In this limit $J_2(\beta,\mu) \simeq 8/\sqrt{\tanh\beta}$. To calculate $m$ and $\eta$ at small values of $\beta$, $\beta \leq 0.3$, it is possible to use the solution (28). In this case a good approximation for $J_2(\beta,\mu)$ can be provided by the formula

$$J_2(\beta,\mu) \simeq \frac{2\pi}{K}\left[\frac{\pi\beta\mu}{K\sin\frac{\pi\beta\mu}{K}}+1\right], \tag{40}$$

where $K$ is determined by the relation (36).

On the other hand, at $\beta \geq 2$ the approximation of "infinitely thick" electrodes is valid when the kernel of the integral equation is represented by the McDonald function (24). Curve 4 exhibits the dependence $J_2(\beta,\mu)$ on $\mu$ in this case. The curves for the dependences $J_2(\beta,\mu)$ for $\beta \geq 2$ coincide completely with this curve. Let us note finally that under large values of $\beta$ and strong nonlocality $\mu \gg 1$ the solution (25) provides a good approximation $J_2(\beta,\mu) \approx 2\pi\mu$ which was found in Ref. 2.

## IV. CONCLUSIONS

Thus, the results obtained permit us to describe vortices which arise in the distributed Josephson junction of a finite electrode thickness. The structure of these vortices varies when the thickness of the electrodes diminishes and depends on the ratio of London and Josephson screening depths. A decrease of the electrode thickness $d$ leads to a shrinking of the vortex. As a consequence of this we have, on the one hand, an increase of its mass and mobility and, on the other hand, a decrease of its energy. When the thickness of the electrodes is $d > 2\lambda_L$ the junction behaves as infinitely thick in both local ($\lambda_L \ll \lambda_j$) and nonlocal limits.

Let us point out that in the case of infinitely thick electrodes the fluxon energy $F$ determines a lower critical field of entry of vortices into the junction, $H_{c1} = 4\pi F/\Phi_0$. When the contact has a finite thickness it is necessary to take into account the penetration of the magnetic field into the electrodes from the outside. When the thickness of the electrodes is finite this leads to a decrease of the Meissner phase volume and, as a consequence, to an increase in the critical field. In thin films the value $H_\infty^0$, being determined by formula (31), plays the role of this critical field. Interference of the Meissner screening currents and those of the magnetic vortex causes a vortex shrinking. Nevertheless, the question of single vortex stability at $H \geq H_\infty^0$ in a Josephson junction of a finite length needs further investigation.

Magnetic vortices of the type discussed can also arise in many-layered structures with thin superconductive interlayers where tunnel current can be extremely large. High-temperature oxide superconductors consisting of weakly coupled superconductive layers corresponding to CuO planes would be regarded as natural examples of structures of such kind (see, for example, Ref. 15) On the other hand, such structures are fabricated nowadays by artificial means, keeping in mind, for example, the potentials of their applications for a generation of microwave radiation. For instance, Ref. 16 deals with an experimental investigation of trilayer Josephson contacts with two extremely thin electrodes of Y-Ba-Cu-O separated by an interlayer of Pr-B-Cu-O. It was found in Ref. 16 that as the thickness of the isolating interlayer decreases, the magnitude of the critical current ceases to obey an exponential dependence which is characteristic for thick interlayers. A possible explanation of this phenomenon would be a drastic drop of the Josephson screening depth. In this connection the appearance of nonlocal magnetostatics in such structures must not be ruled out.

In conclusion let us make one remark about the possible conditions for the appearance of these vortices in many-layered structures. It is known that the magnetic field can penetrate into a structure both in the form of the vortices within one junction, discussed above, and in the form of "hypervortices" which cover several weakly coupled layers simultaneously.[17] The form and sizes of such hypervortices are determined by averaged London screening depths with respect to longitudinal and transversal directions. A critical field of entry of the hypervortex into the layered structure is determined by the energy of these formations. But when pinning of the hypervortex is large or when the size of the structure is comparable with the size of the hypervortex, the magnetic field can generate vortices within individual junctions. Such a situation was demonstrated in Ref. 12 in a numerical investigation of layered structures of this kind.

## ACKNOWLEDGMENTS

The authors are grateful to Professor V. Eleonsky, Professor V. Silin, and Professor Yu. Aliev for useful discussions and to Dr. A. Gundarin and Dr. V. Korolev for help in their work. This research was supported by grants from the International Science Foundation (R0500) and the Russian Foundation for Basic Researchs (95-01-00060).

## APPENDIX

To analyze qualitatively Eq. (21) it turns out to be convenient to use an approach of Ref. 14. This approach involves a replacing of the initial integro-differential equation by a system of ordinary differential equations. The order of this system is determined by the kernel of the integral operator and may be infinite. In so doing it is possible to regard the initial integro-differential equation as a dynamic system with respect to the spatial variable. The solutions $\varphi = 2\pi n, n \in \mathbb{Z}$, represent singular points (equilibrium states) of this system. The fluxon soluton corresponds to a special trajectory of the dynamic system which emerges from the unstable equilibrium state $\varphi = 0$ and goes into another equilibrium state $\varphi = 2\pi$.

Let us show the way to introduce a dynamic system which corresponds to (21). We use the representation (20) for the kernel $G_\beta(v)$,

$$G_\beta(v) = \frac{1}{\beta}\sum_{n=0}^{\infty}\frac{e^{-\omega_n|v|}}{\omega_n},$$
$$\omega_n = \sqrt{1+\left(\frac{\pi}{2\beta}\right)^2(1+2n)^2}, \tag{A1}$$

and introduce the auxiliary functions

$$q_n(w) = \frac{\omega_n}{2\mu}\int_{-\infty}^{\infty}\exp\left\{-\frac{\omega_n|w-u|}{\mu}\right\}\frac{d\varphi}{du}du, \quad n = 0,1,\ldots. \tag{A2}$$

It is evident that each of them satisfies the equation

$$-\frac{\mu^2}{\omega_n^2}\frac{d^2q_n}{dw^2} + q_n = \frac{d\varphi}{dw}, \qquad n = 0,1,\ldots. \tag{A3}$$

Equation (21) can be rewritten in the form

$$\sin\varphi = \frac{1}{\mu}\int_{-\infty}^{\infty}G_\beta\left(\frac{|w-u|}{\mu}\right)\frac{d^2\varphi}{du^2}du = \frac{2}{\beta}\sum_{n=0}^{\infty}\frac{1}{\omega_n^2}\frac{dq_n}{dw}. \tag{A4}$$

Thus, Eq. (21) can be represented as the infinite system (A3),(A4) of differential equations for the initial variable $\varphi$ and an infinite number of the auxiliary variables $q_n$.

A simple consequence of this representation is the existence of the integral (32). To obtain it it is sufficient to multiply Eq. (A4) by $d\varphi/dw$, to multiply Eqs. (A3) by $-(2/\beta\omega_n^2)\,dq_n/dw$, and to sum up these equations. Being expressed in terms of the auxiliary variables $q_n$, $n = 0,1\ldots$, the first integral takes the form

$$I = (1-\cos\varphi) + \sum_{n=0}^{\infty}\frac{\mu^2}{\beta\omega_n^4}\left(\frac{dq_n}{dw}\right)^2 - \sum_{n=0}^{\infty}\frac{1}{\beta\omega_n^2}q_n^2. \tag{A5}$$

It is easy to rewrite it in the form of (32) using the explicit expression (A2) for $q_n$.

* Electronic address: anadep@fp.elvis.msk.su


[1] Yu.M. Aliev, V.P. Silin, and S.A. Uryupin, Superconductivity **5**, 230 (1992); [Sverkhprovodimost Fiz. Khim. Tekh. **5**, 228 (1992)].
[2] A. Gurevich, Phys. Rev. B. **46**, 3187 (1992).
[3] V.P. Silin, JETP Lett. **58**, 701 (1993).
[4] Yu.M. Aliev and V.P. Silin, J. Exp. Theor. Phys. **77**, 142 (1993).
[5] G.L. Alfimov and V.P. Silin, J. Exp. Theor. Phys. **79**, 369 (1994).
[6] A. Gurevich, Phys. Rev. B **48**, 12 857 (1993).
[7] Yu.M. Ivanchenko and T.K. Soboleva, Phys. Lett. A **147**, 65 (1990).
[8] R.G. Mints and I.B. Snapiro, Phys. Rev. B **49**, 6188 (1994).
[9] M.H. Tinkham, Phys. Rev. **129**, 2413 (1963).
[10] M. Weihnacht, Phys. Status Solidi **32**, K169 (1969).
[11] G.L. Alfimov and V.P. Silin, Phys. Lett. A **198**, 105 (1995).
[12] R. Kleiner, P. Muller, H. Kohlstedt, N.F. Pedersen, and S. Sakai, Phys. Rev. B **50** 3942 (1994).
[13] A. Seeger, *Theorie der Gitterfehlstellen*, Handbuch der Physik Vol. 7(1) (Springer, Berlin, 1955), p. 383.
[14] G.L. Alfimov, V.M. Eleonsky, and N.E. Kulagin, Chaos **2**, 565 (1992).
[15] L.N. Bulaevskii, J.R. Clem, and L.I. Glazman, Phys. Rev. B **46**, 350 (1992); L.N. Bulaevskii, V.G. Kogan, and M. Ledvij, *ibid.* **46**, 366 (1992).
[16] B. Ghyselen, M.A. Bari, E.J. Tarte, M.G. Blamire, R.E. Somekh, Y. Yan, and J.E. Evetts, J. Phys. C **230**, 327 (1994).
[17] M.V. Fistul' and G.F. Giuliani, J. Phys. C **230**, 9 (1994).